

VERTICAL EMITTANCE MEASUREMENT AT THE ESRF

F. Ewald, P. Elleaume, L. Farvacque, A. Franchi, D. Robinson, K. Scheidt, A. Snigirev, I. Snigireva, ESRF, Grenoble, FRANCE

Abstract

In the short term the ESRF aims to reach emittances of less than 2 pm. We review the existing emittance diagnostics – X-ray projection monitors and pinhole cameras – and evaluate their ability to resolve such ultra-small vertical emittances. Even though these devices are reliable and show good agreement between measurements and theoretical predictions down to vertical emittance values of less than 10 pm, they will reach their limit of resolution for emittances decreasing below a few picometers. In addition to the existing emittance diagnostics, a new device was installed that images bending magnet radiation using compound refractive lenses (CRLs).

REVIEW OF VERTICAL EMITTANCE DIAGNOSTICS AT THE ESRF

Simulations show that increasing the number of skew quadrupoles can improve the vertical emittance in the ESRF storage ring. As a consequence of this upgrade which was done a few months ago, the ESRF is currently operated with vertical emittances between 3 and 5 pm at 200 mA (7/8 + 1 filling mode). Even smaller vertical emittances of down to 2 pm are predicted [1]. This is the occasion to review the existing vertical emittance measurement devices and to evaluate their ability to resolve such ultra-small emittances.

Currently, the emittance in the ESRF storage ring is measured and continuously monitored using two different methods in parallel: Imaging of bending magnet radiation with a pinhole camera [2], and detection of projected dipole radiation [3]. Their benefits and limitations will be briefly discussed in the following section. A complementary setup, based on X-ray lens imaging, has recently been installed. It will be presented in the second section together with first results.

Detection of Projected Dipole Radiation

11 dipole radiation projection monitors [3] are installed in air behind the X-ray beam absorber of the second dipole of a cell. These very compact devices take advantage of very high energy synchrotron radiation (166 keV) leaking through the absorbers. The interest of having so many devices evenly distributed around the storage ring is twofold: First, the monitoring of the vertical emittance at many different positions along the storage ring allows to appreciate its modulation around the circumference s due to coupling, and comparison with the theoretical machine model

for $\varepsilon(s)$. Second, the large number of devices is used to calculate an average vertical emittance, which resolves smallest emittance variations in the order of $\Delta\varepsilon \approx 0.05$ pm. The measurement of small absolute vertical emittance values with these devices is, however, strongly dominated and limited by the divergence of synchrotron radiation. At a photon energy of 166 keV, the synchrotron radiation has an rms-divergence of $17.5 \mu\text{rad}$. Thus, its contribution to the beam size at the position of the detector is $31.5 \mu\text{m}$. For emittances of 30 pm the electron beam size equals the synchrotron radiation contribution, while at the currently delivered emittances of roughly 4 pm the electron beam accounts only for 30%, i.e. $11.8 \mu\text{m}$, of the total beam size on the screen. Thus, the deconvolution of electron beam size and synchrotron radiation becomes prone to errors at small emittances. Comparing the measurements with the machine model shows that the dipole radiation projection monitors are reliable for absolute emittance measurements down to 15 pm. Below, the measurements do not follow the model, indicating influences of alignment uncertainties that become critical at very low emittances, such as the source distance. Consequently, an absolute measurement of ultra-small emittances with these devices is only possible after careful review of the device alignment and after calibration with other measurements.

Pinhole Camera

Two pinhole cameras are installed in the storage ring (at beam ports ID25 and D9). Their working principle is described in detail in [2]. The resolution of an X-ray pinhole camera is determined by its geometrical aperture and by the resolution of the visible light detection unit (scintillator, lenses, CCD). The latter can be measured and minimised by using thin scintillators and appropriate aberration-free imaging optics. Concerning the pinhole itself, a large aperture will lead to image blurring by the geometrical projection of the pinhole opening. The contribution to the total measured beam size by this effect is [2]

$$\sigma_A = A_{\text{ph}} \frac{D+d}{d} \frac{1}{\sqrt{12}} \quad , \quad (1)$$

where the factor $1/\sqrt{12}$ is due to the conversion of the width of the rectangular profile to an rms-value σ_A . d and D are the distances between source and pinhole and pinhole and screen, respectively. A_{ph} is the vertical pinhole aperture. The effect of blurring the image by geometrical projection through a finite pinhole size can thus be minimised by reducing the pinhole aperture. But, when reach-

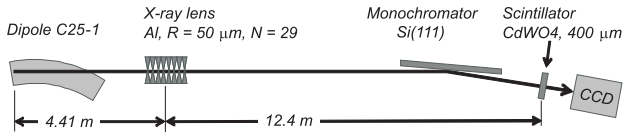


Figure 1: Sketch of the refractive lens setup.

ing small apertures, diffraction will occur. In the limit of Fraunhofer diffraction, i.e. for very small pinholes, the contribution from diffraction to the total beam size can be expressed by the size of the Airy-spot:

$$\sigma_{\text{diff}} = 0.61\lambda D/A_{\text{ph}} \quad (2)$$

The total point spread function of the pinhole can then be expressed as $\sigma_{\text{psf}} = \sqrt{\sigma_{\text{A}}^2 + \sigma_{\text{diff}}^2}$, and an optimum pinhole size $A_{\text{ph}}^{\text{opt}}$ and the corresponding minimum spot size on the screen $\sigma_{\text{psf}}^{\text{min}}$ can be derived:

$$A_{\text{ph}}^{\text{opt}} = \sqrt{\frac{3.66\lambda d D}{D+d}}, \quad \sigma_{\text{psf}}^{\text{min}} = 0.6\sqrt{\frac{\lambda D(D+d)}{d}} \quad (3)$$

The pinhole setup at the ID25 beam port has the following parameters: $\lambda = 12.4$ pm, $d = 4.17$ m, $D = 12.04$ m. Hence, $A_{\text{ph}}^{\text{opt}} = 10$ μm , $\sigma_{\text{psf}}^{\text{min}} = 14$ μm , and the corresponding emittance value that limits the resolution of the pinhole system is $\varepsilon_{\text{psf}}^{\text{min}} \approx 0.5$ pm. For a more precise treatment of the pinhole resolution, Fresnel diffraction from the pinhole [4] and convolution with the electron beam size has to be taken into account. Such a correct treatment yields very similar results [5].

EMITTANCE MEASUREMENT USING X-RAY LENSES

An emittance diagnostics using parabolic compound refractive lenses (CRLs) was installed recently at the beam port of ID25. X-ray lenses made of aluminium and beryllium become more and more common in synchrotron radiation applications ([6] and references therein). Their benefits are easy alignment and excellent imaging quality. The new setup uses the same source point as the pinhole camera. In this way, either the pinhole or the X-ray lens can be moved into the X-ray beam, and direct comparisons of the measurements can be made. The lens itself is placed at a distance of $d_{\text{L}} = 4.4$ m from the source point (figure 1). At $D_{\text{L}} = 12.4$ m from the CRL the X-ray spot is imaged by a conventional X-ray imaging system using a 500 μm thick CdWO_4 scintillator, a double achromat and a CCD camera (Flea from Point Grey Research). Since lenses for X-rays show chromatic aberration, a Si(111) monochromator in Laue geometry is used to select the desired photon energy. In our setup the source distance d_{L} and the image distance D_{L} to the lens are fixed, and the needed focal distance is therefore $f = 3.25$ m. The focal distance of a CRL lens stack for X-rays is determined by the choice of material, radius of curvature R in the apex of the parabolically shaped

lens, the number N of single lenses combined in a stack and the photon energy E [6]:

$$f = R/2N\delta(E) \quad (4)$$

δ is the material dependent decrement of the index of refraction that takes the form $n = 1 - \delta + i\beta$ for X-rays. Following this relation, the focal length of a lens stack can be controlled. Since our beam port exit window is made of 3 mm aluminium which absorbs a large part of the low energy dipole radiation, we work at high photon energies ≥ 25 keV and use aluminium lenses.

The theoretical resolution of our CRL imaging setup is only determined by diffraction from the lens aperture. The effective aperture (physical aperture taking into account the radially increasing absorption in the lens material) of a parabolic lens with a radius of curvature of 50 μm made from a 1 mm thick Aluminium sheet is $A_{\text{L}}^{\text{eff}} \approx 300$ μm . The diffraction limited resolution of the source point is then $1.22\lambda f/A_{\text{L}}^{\text{eff}} \approx 0.5$ μm at a photon energy of 35 keV. Let us now assume a vertical emittance of 1 pm, then this translates into a vertical beam size of $\sigma = \sqrt{\varepsilon\beta} \approx 7$ μm at the source point of the CRL setup ($\beta = 47.65$ m). Thus, the resolution of the setup is largely sufficient to resolve the expected ultra-small vertical emittances. In the following, the results of the first measurements with the new CRL setup will be presented.

Comparison of Aluminium and Beryllium Lenses

Lenses made of aluminium and beryllium ($R = 50$ μm) were compared to each other at two different energies: 35 keV and 45 keV. Figure 2 shows the comparison of vertical beam profiles measured with aluminium and beryllium lenses. The profiles show a halo in case of imaging with the beryllium lenses, which is attributed to the geometric opening of the lens: the vertical *rms*-beam size at the position of the lens is roughly $150 - 200$ μm . Thus, the beam just matches the geometrical lens opening of 222 μm . Nevertheless, the wings of the beam are extended beyond the geometrical lens opening. This part of the beam is transmitted straight through the bulk material in which the lens is printed without being subject to focusing. It therefore appears as a halo around the image spot. The halo intensity depends on the absorption of the observed X-rays in the lens material. Since beryllium has a higher transmission than aluminium, this effect is stronger in beryllium than in aluminium. Adding an absorbing diaphragm of the size of the geometrical lens opening in front of the lens stack should avoid this halo.

Aluminium Lenses at Different Photon Energies

Figure 3 shows vertical beam profiles taken at different photon energies. The number N of single lens elements was changed, and the according energy selected with the monochromator crystal. At lower energies, notably at 25 keV, a strong background contributes to the profile,

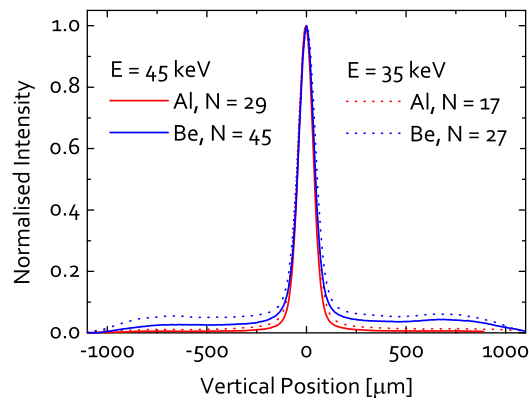


Figure 2: Vertical beam profiles recorded with different sets of lenses: Be (blue) and Al (red) at two photon energies 35 keV (dotted) and 45 keV (plain).

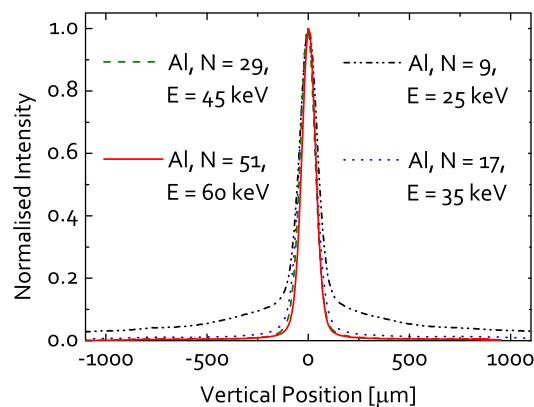


Figure 3: Vertical profiles for imaging with aluminium lenses at different energies.

while it is significantly reduced at energies ≥ 45 keV. Different effects may contribute to this background: At 25 keV, a contribution from the 3rd harmonic reflection was clearly identified. At higher energies the 3rd harmonic has less weight since its contribution drops with the reduced flux of the synchrotron radiation spectrum at high energies. Furthermore, small angle scattering originating from the UHV beam port window (3 mm aluminum of unknown purity and grain structure) is identified to contribute to the background. With increasing photon energy this contribution is reduced since the scattering angle narrows down with higher energies. Small angle scattering from the lens material itself does not seem to contribute to the observed background.

Comparison of Pinhole and Lens Setups

In figure 4 the emittance values measured with the lens are plotted against those obtained from the pinhole camera that is observing the same source point. For all tested configurations, such as lens material, X-ray energy, radius of curvature, monochromator crystal, the vertical emittance values deduced from the measurements with the X-ray lens

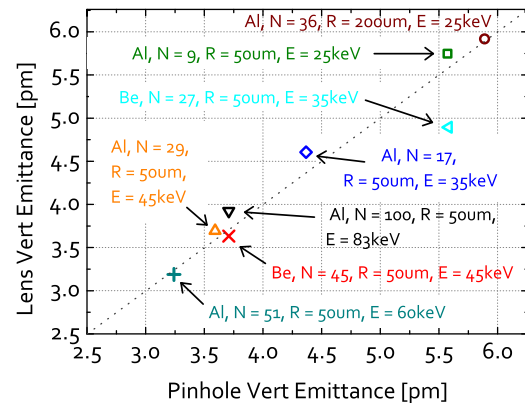


Figure 4: Comparison of different vertical emittances measured with the CRL setup and the pinhole under different experimental conditions.

and those measured with the pinhole camera are in very good agreement. The only point that fits less is the beryllium lens at 35 keV. As the Be-lenses show a very high background as discussed above, this may have introduced an error in the beam size measurement.

CONCLUSIONS

The pinhole cameras as well as the recently installed X-ray lens imaging system are very well capable of resolving the small vertical emittances of less than 4 pm, delivered currently in the ESRF storage ring. The resolution of both devices is furthermore largely sufficient to resolve the predicted ultra-small vertical emittances of ≤ 2 pm.

The dipole radiation projection monitors reach their limit for an absolute emittance measurement below 10 pm. They remain, however, a very sensitive diagnostics to detect smallest vertical emittance variations even at the currently delivered emittances of ≤ 4 pm.

REFERENCES

- [1] A. Franchi, *et al.*, “Vertical Emittance Reduction and Preservation at the ESRF Electron Storage Ring” Proceedings of IPAC’11, TU00DA01, to be published.
- [2] P. Elleaume, *et al.*, “Measuring Beam Sizes and Ultra-Small Electron Emittances Using an X-ray Pinhole Camera” J. Synchrotron Rad. 2 (1995) 209.
- [3] B. K. Scheidt, “Measurement of vertical emittance with a system of six -In-Air-X-Ray- projection monitors at the ESRF” DIPAC’07, Venice, 2007, TUPB08, p. 72.
- [4] C. Thomas, *et al.*, “X-ray pinhole camera resolution and emittance measurement” Phys. Rev. ST Accel. Beams 13 (2010) 022805.
- [5] P. Elleaume, “Emittance Determination from a Pinhole Camera” Internal Report ESRF 10-01/Diagnostics
- [6] B. Lengeler, *et al.*, “Parabolic refractive X-ray lenses: a breakthrough in X-ray optics” Nucl. Instr. and Meth. in Phys. Res. A 467–468 (2001) p. 944.